BOSTER
antibody and ELISA experts

BOSTER BIOLOGICAL TECHNOLOGY
3942 B Valley Ave, Pleasanton, CA 94566
888-466-3604 | support@bosterbio.com | www.bosterbio.com

Anti-CD11b ITGAM Rabbit Monoclonal Antibody

Catalog Number: M00144-1

Overview

Product Name	Anti-CD11b ITGAM Rabbit Monoclonal Antibody
Reactive Species	Human, Mouse, Rat
Description	Boster Bio Anti-CD11b ITGAM Rabbit Monoclonal Antibody catalog # M00144-1. Tested in WB, IHC, ICC/IF applications. This antibody reacts with Human, Mouse, Rat.
Application	IF, IHC, ICC, WB
Clonality	Monoclonal GC-9
Formulation	Rabbit IgG in stabilizing components, phosphate buffered saline, pH 7.4, 150mM NaCl, 0.02% sodium azide and 50% glycerol. *This antibody is supplied in a stabilized formulation. Compatibility with conjugation reactions depends on the chemistry of the conjugation method used. For conjugation methods that are not compatible with the stabilizing components present in this formulation, a carrier-free antibody format is required.
Storage Instructions	Store at -20°C for one year. For short term storage and frequent use, store at 4°C for up to one month. Avoid repeated freeze-thaw cycles.
Host	Rabbit
Uniprot ID	P11215

Technical Details

Immunogen	A synthesized peptide derived from human CD11b
Isotype	Rabbit IgG
Form	Liquid
Concentration	0.5mg/ml
Purification	Affinity-chromatography
Suggested Dilutions	WB 1:500-2000 IHC 1:50-200 ICC/IF 1:50-200

BOSTER BIOLOGICAL TECHNOLOGY
3942 B Valley Ave, Pleasanton, CA 94566
888-466-3604 | support@bosterbio.com | www.bosterbio.com

Anti-CD11b ITGAM Rabbit Monoclonal Antibody (M00144-1) Images

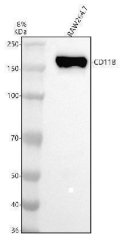

Western blot analysis of CD11B/Integrin Alpha M/ITGAM using anti-CD11B/Integrin Alpha M/ITGAM antibody (M00144-1). Electrophoresis was performed on a 5-20% SDS-PAGE gel at 70V (Stacking gel) / 90V (Resolving gel) for 2-3 hours. The sample well of each lane was loaded with 30 ug of sample under reducing conditions. Lane 1: mouse RAW264.7 whole cell lysates.After electrophoresis, proteins were transferred to a nitrocellulose membrane at 150 mA for 50-90 minutes. Blocked the membrane with 5% non-fat milk/TBS for 1.5 hour at RT. The membrane was incubated with rabbit anti-CD11B/Integrin Alpha M/ITGAM antigen affinity purified monoclonal antibody (M00144-1) at 1:500 overnight at 4°C, then washed with TBS-0.1%Tween 3 times with 5 minutes each and probed with a goat anti-rabbit IgG-HRP secondary antibody at a dilution of 1:5000 for 1.5 hour at RT. The signal is developed using an Enhanced Chemiluminescent detection (ECL) kit (Catalog # EK1002) with Tanon 5200 system. A specific band was detected for CD11B/Integrin Alpha M/ITGAM at approximately 170 kDa. The expected band size for CD11B/Integrin Alpha M/ITGAM is at 127 kDa.

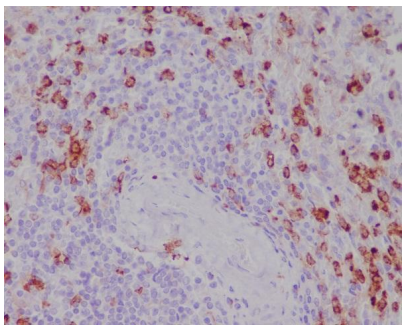

Immunohistochemical analysis of paraffin-embedded human spleen, using CD11b Antibody.

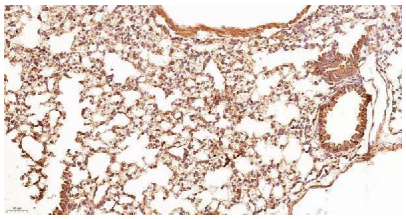

Immunohistochemical analysis of paraffin-embedded mouse lung, using CD11b Antibody.

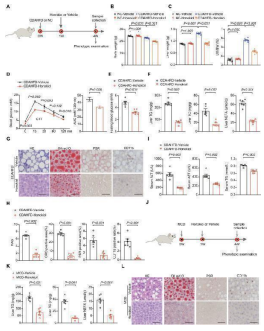

Honokiol protects against mouse NASH. A Schematic of the CDAHFD-induced NASH model and evaluating the therapeutic effects of honokiol in vivo (100 mg/kg). B Body weights of NC- or CDAHFD-fed mice treated with honokiol or vehicle three weeks after subjecting them to their respective diets for one week. n = 6 mice per group. One-way ANOVA was used for statistical analysis. C Liver weights and ratio of liver weight to body weight (LW/BW) of NC- or CDAHFD-fed mice treated with honokiol or CMC three weeks after subjecting them to their respective diets for one week. n = 6 mice per group. One-way ANOVA assay was used for statistical analysis. D Blood glucose concentrations during

BOSTER BIOLOGICAL TECHNOLOGY
3942 B Valley Ave, Pleasanton, CA 94566
888-466-3604 | support@bosterbio.com | www.bosterbio.com

GTT and the AUC of GTT of CDAHFD-fed mice treated with vehicle or honokiol. E Fasting blood glucose (FBG) concentrations of CDAHFD-fed mice treated with vehicle or honokiol. n = 6 mice per group. Student's t -test was applied for statistical analysis. F TG, TC and NEFA levels in the livers of CDAHFD-fed mice treated with honokiol or vehicle. n = 6 mice per group. Student's t -test was applied for statistical analysis. G Representative images of indicated mouse liver sections stained with HE, ORO, PSR, and IHC for CD11b-positive cells. n = 6 mice per group. Scale bar 50 um. H Results of NAS (HE) and quantitative analysis of ORO, PSR, and CD11b shown in (G). n = 6 mice per group. The Mann–Whitney U test was used for NAS and Student's t -test was applied to ORO, PSR, and CD11b data. I Serum ALT and AST activity and serum TG concentrations in CDAHFD-fed mice treated with honokiol or vehicles. n = 6 mice per group. Student's t -test was applied for statistical analysis. J Schematic of the MCD-induced NASH model and evaluating the therapeutic effects of honokiol in vivo (100 mg/kg). K TG, TC. and NEFA levels in the livers of MCD-fed mice treated with honokiol or vehicle. n = 6 mice per group. Student's t -test was applied for statistical analysis. L Representative images of the indicated mouse liver sections stained with HE, ORO, PSR, and IHC for CD11b-positive cells. n = 6 mice per group. Scale bar 50 um. M Results of NAS (HE) and quantitative analysis of ORO, PSR, and CD11b data shown in (L) . n = 6 mice per group. For statistical analysis, the Mann–Whitney U test was used for NAS and Student's t -test was applied to ORO, PSR, and CD11b. N Serum ALT and AST activity of MCD-fed mice treated with honokiol or vehicle. n = 6 mice per group. Student's t -test was applied for statistical analysis. O GSVA pathway enrichment analysis related to cell damage and death, inflammation, lipid metabolism, and fibrosis differentially regulated by honokiol treatment. n = 5 mice per group. P Heatmaps of gene expression profiles involved in cell damage and death, lipid metabolism, inflammation, and fibrosis Index in PubMed under a CC BY license. PMID: 36932412

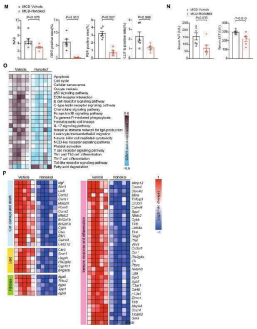

Honokiol protects against mouse NASH. A Schematic of the CDAHFD-induced NASH model and evaluating the therapeutic effects of honokiol in vivo (100 mg/kg). B Body weights of NC- or CDAHFD-fed mice treated with honokiol or vehicle three weeks after subjecting them to their respective diets for one week. n = 6 mice per group. One-way ANOVA was used for statistical analysis. C Liver weights and ratio of liver weight to body weight (LW/BW) of NC- or CDAHFD-fed mice treated with honokiol or CMC three weeks after subjecting them to their respective diets for one week. n = 6 mice per group. One-way ANOVA assay was used for statistical analysis. D Blood glucose concentrations during GTT and the AUC of GTT of CDAHFD-fed mice treated with vehicle or honokiol. E Fasting blood glucose (FBG) concentrations of CDAHFD-fed mice treated with vehicle or honokiol. n = 6 mice per group. Student's t -test was applied for statistical analysis. F TG, TC and NEFA levels in the livers of CDAHFD-fed mice treated with honokiol or vehicle. n = 6 mice per group. Student's t -test was applied for statistical analysis. G Representative images of indicated mouse liver sections stained with HE, ORO, PSR, and IHC for CD11b-

BOSTER BIOLOGICAL TECHNOLOGY
3942 B Valley Ave, Pleasanton, CA 94566
888-466-3604 | support@bosterbio.com | www.bosterbio.com

positive cells. n = 6 mice per group. Scale bar 50 um. H Results of NAS (HE) and quantitative analysis of ORO, PSR, and CD11b shown in (G). n = 6 mice per group. The Mann–Whitney U test was used for NAS and Student's t -test was applied to ORO, PSR, and CD11b data. I Serum ALT and AST activity and serum TG concentrations in CDAHFD-fed mice treated with honokiol or vehicles. n = 6 mice per group. Student's t -test was applied for statistical analysis. J Schematic of the MCD-induced NASH model and evaluating the therapeutic effects of honokiol in vivo (100 mg/kg). K TG, TC. and NEFA levels in the livers of MCD-fed mice treated with honokiol or vehicle. n = 6 mice per group. Student's t -test was applied for statistical analysis. L Representative images of the indicated mouse liver sections stained with HE, ORO, PSR, and IHC for CD11b-positive cells. n = 6 mice per group. Scale bar 50 um. M Results of NAS (HE) and quantitative analysis of ORO, PSR, and CD11b data shown in (L) . n = 6 mice per group. For statistical analysis, the Mann–Whitney U test was used for NAS and Student's t -test was applied to ORO, PSR, and CD11b. N Serum ALT and AST activity of MCD-fed mice treated with honokiol or vehicle. n = 6 mice per group. Student's t -test was applied for statistical analysis. O GSVA pathway enrichment analysis related to cell damage and death, inflammation, lipid metabolism, and fibrosis differentially regulated by honokiol treatment. n = 5 mice per group. P Heatmaps of gene expression profiles involved in cell damage and death, lipid metabolism, inflammation, and fibrosis Index in PubMed under a CC BY license. PMID: 36932412

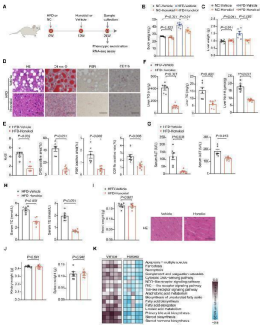

Honokiol ameliorates high fat diet (HFD)-induced non-alcoholic fatty liver disease. A Schematic showing HFD-induced NAFLD and evaluation of therapeutic effects of honokiol in vivo (100 mg/kg). B and C Body (B) and liver weight (C) of NC- or HFD-fed mice treated with honokiol or vehicle after 12 weeks of their respective diets. n = 6 mice per group. One-way ANOVA was used for statistical analysis. D Representative images of indicated mouse liver sections stained with hematoxylin and eosin (HE), oil red O (ORO), picrosirius red (PSR), and immunohistochemistry (IHC) of CD11b-positive cells. n = 6 mice per group. Scale bar 50 um. E Results of NAS (HE) and quantitative analysis of ORO, PSR, and CD11b shown in (D). n = 6 mice per group. Mann–Whitney U test was used for NAS, while Student's t -test was applied to ORO, PSR, and CD11b data. F TG, TC, and non-esterified fatty acids (NEFA) in the livers of HFD-fed mice treated with honokiol or vehicle after 12 weeks of their respective diets. n = 6 mice per group. Student's t -test was applied for statistical analysis. G Serum ALT and AST activity in HFD-fed mice treated with honokiol or vehicle after 12 weeks of their respective diets. n = 6 mice per group. Student's t -test was applied for statistical analysis. H Serum TC and TG concentrations in HFD-fed mice treated with honokiol or vehicle after 12 weeks of their respective diets. n = 6 mice per group. Student's t -test was applied for statistical analysis. I Heart weights and heart histological staining of HFD-fed mice treated with honokiol or vehicle after 12 weeks of their respective diets. n = 6 mice per group. Student's t -test was applied for statistical analysis. Scale bar 50 um. J Kidney and spleen weights of HFD-fed

BOSTER BIOLOGICAL TECHNOLOGY
3942 B Valley Ave, Pleasanton, CA 94566
888-466-3604 | support@bosterbio.com | www.bosterbio.com

mice treated with honokiol or vehicle after 12 weeks of their respective diets. n = 6 mice per group. Student’s t -test was applied for statistical analysis. K GSVA enrichment analysis related to inflammation, lipid metabolism, and fibrosis downregulated by honokiol treatment. n = 5 mice per group. L Heatmap of gene expression profiles involved in cell damage and death, inflammation, and lipid metabolism. n = 5 mice per group Index in PubMed under a CC BY license. PMID: 36932412

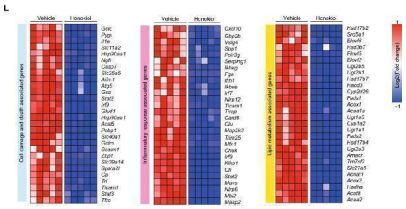

Honokiol ameliorates high fat diet (HFD)-induced non-alcoholic fatty liver disease. A Schematic showing HFD-induced NAFLD and evaluation of therapeutic effects of honokiol in vivo (100 mg/kg). B and C Body (B) and liver weight (C) of NC- or HFD-fed mice treated with honokiol or vehicle after 12 weeks of their respective diets. n = 6 mice per group. One-way ANOVA was used for statistical analysis. D Representative images of indicated mouse liver sections stained with hematoxylin and eosin (HE), oil red O (ORO), picrosirius red (PSR), and immunohistochemistry (IHC) of CD11b-positive cells. n = 6 mice per group. Scale bar 50 um. E Results of NAS (HE) and quantitative analysis of ORO, PSR, and CD11b shown in (D). n = 6 mice per group. Mann–Whitney U test was used for NAS, while Student’s t -test was applied to ORO, PSR, and CD11b data. F TG, TC, and non-esterified fatty acids (NEFA) in the livers of HFD-fed mice treated with honokiol or vehicle after 12 weeks of their respective diets. n = 6 mice per group. Student’s t -test was applied for statistical analysis. G Serum ALT and AST activity in HFD-fed mice treated with honokiol or vehicle after 12 weeks of their respective diets. n = 6 mice per group. Student’s t -test was applied for statistical analysis. H Serum TC and TG concentrations in HFD-fed mice treated with honokiol or vehicle after 12 weeks of their respective diets. n = 6 mice per group. Student’s t -test was applied for statistical analysis. I Heart weights and heart histological staining of HFD-fed mice treated with honokiol or vehicle after 12 weeks of their respective diets. n = 6 mice per group. Student’s t -test was applied for statistical analysis. Scale bar 50 um. J Kidney and spleen weights of HFD-fed mice treated with honokiol or vehicle after 12 weeks of their respective diets. n = 6 mice per group. Student’s t -test was applied for statistical analysis. K GSVA enrichment analysis related to inflammation, lipid metabolism, and fibrosis downregulated by honokiol treatment. n = 5 mice per group. L Heatmap of gene expression profiles involved in cell damage and death, inflammation, and lipid metabolism. n = 5 mice per group Index in PubMed under a CC BY license. PMID: 36932412

Laptm5 -HKO exacerbates HFHC-induced NASH. a Fasting blood glucose of Laptm5 -HKO and Laptm5 -Flox mice for NC or HFHC consumptions (n = 10 mice/group). b and c Liver weight and LW/BW (b), and hepatic TG, TC contents (c) of Laptm5 -HKO and Laptm5 -Flox mice after NC or HFHC feeding for 8 or 16 weeks (n = 10 mice/group). d H&E (upper) and Oil Red O (lower) staining in the liver sections of mice in the indicated groups (n = 6 mice/group). Scale bar,

BOSTER BIOLOGICAL TECHNOLOGY
3942 B Valley Ave, Pleasanton, CA 94566
888-466-3604 | support@bosterbio.com | www.bosterbio.com

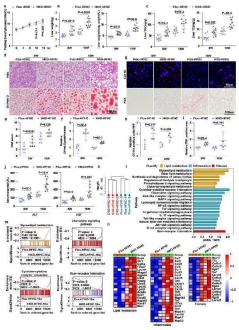

100 um. e and f NAS score analysis (e) and the statistical analysis of Oil red O staining (f) of Laptm5 -HKO and Laptm5 -Flox mice after NC or HFHC feeding for 8 or 16 weeks (n = 6 mice/group). g Immunofluorescence staining (g) and statistical analysis (h , i) of CD11b (red) in the liver sections of mice in the indicated groups. (Nuclei, blue) (n = 4 mice/group). Scale bar, 50 um. PSR staining of mice liver sections in the indicated groups. (8 weeks, n = 6 mice/group, 16 weeks, n = 7 Laptm5 -Flox mice and n = 5 Laptm5 -HKO mice). Scale bars, 100 um. j Serum ALT and AST concentrations of mice in the indicated groups (n = 10 mice/group). k Hierarchical clustering analysis of the RNA-seq data from the mice fed the HFHC diet. l and m GSEA pathway enrichment analysis of pathways related to lipid metabolism, inflammation, apoptosis, and fibrosis. n Heatmaps of the genes related to lipid metabolism, inflammatory responses, and fibrosis (red, upregulated; blue, downregulated) in the indicated groups. Data are represented as mean ± SD. The Mann–Whitney U nonparametric statistical test was used for statistical analysis in (c —8w, e —16w, and i —16w) and two-tailed Student’s t -test in other panels. Source data are provided as a Source data file. Index in PubMed under a CC BY license. PMID: 37156795

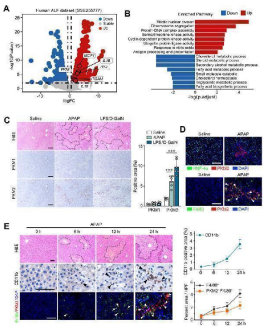

Macrophage PKM2 expression was markedly upregulated in liver tissues with ALI. (A) Log ratio–average (M–A) plots showing the changes in gene expression in ALF patients and control individual (GSE255777). (B) Gene set enrichment analysis (GSEA) of the DEGs. (C) Representative images and quantification of H&E- and immunohistochemistry staining of PKM1 and PKM2 in liver tissues of APAP- or LPS/D-GaIN-induced ALI mice and control mice. (D) Dual immunofluorescence staining for PKM2 and HNF-4alpha (A) or F4/80 (B) in liver tissues of APAP-induced ALI mice and control mice. (E) Representative images of H&E staining, dual immunofluorescence staining for PKM2 and F4/80, and immunohistochemistry staining for CD11b in APAP-induced mouse ALI at the indicated time points with quantification. Scale bar: 100 um. White arrows indicate PKM2 + F4/80 + cells; Necrotic region was enclosed in dotted lines. *** P < 0.001. Error bars depict the standard deviations.Index in PubMed under a CC BY license. PMID: 40351417

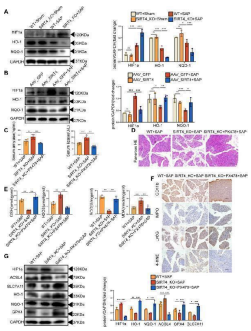

The regulatory effect of SIRT4 on ferroptosis in SAP depends on the HIF-1alpha/HO-1 pathway. A – B The protein expression levels of HIF-1alpha, HO-1 and NQO-1 in the pancreas of mice. C Serum amylase level and lipase activity of mice in different groups after using HIF-1alpha inhibitor PX478 (100 mg/kg). D Representative HE staining images of mice pancreas in different groups after using HIF-1alpha inhibitor PX478 (100 mg/kg). Scale bar = 100 μm. E The levels of oxidative stress factors (GSH, H 2 O 2 , SOD, MDA) in the pancreas of mice in different groups after using HIF-1alpha inhibitor PX478 (100 mg/kg). F Representative IHC staining of CD11b, MPO, Ly6G and 4-HNE in the pancreas of mice in different groups after using HIF-1alpha inhibitor PX478(100 mg/kg). Scale bar = 100 μm. G The

BOSTER BIOLOGICAL TECHNOLOGY
3942 B Valley Ave, Pleasanton, CA 94566
888-466-3604 | support@bosterbio.com | www.bosterbio.com

protein expression level of HIF-1alpha, HO-1, NQO-1, ACSL, GPX4 and SLC7A11 in the pancreas of mice in different groups after using HIF-1alpha inhibitor PX478 (100 mg/kg). WT + SAP group, SIRT4_KO + SAP group, SIRT4_KO + PX478 + SAP group. A – G used GAPDH as the reference protein. * P

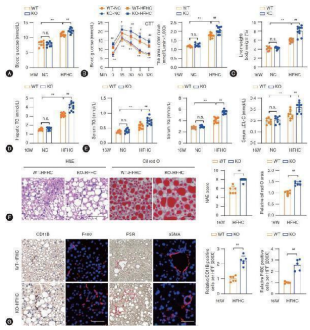

USP29 knockout accelerates hepatic steatosis, inflammation and fibrosis induced by a HFHC diet. (A) blood glucose of WT and USP29-KO mice after NC or HFHC diet treatment for 16weeks (n=8–10 mice/group). (b) GTTs of WT mice and USP29-KO mice were analyzed at the week 15 fed NC chow or HFHC diet (n=8–10 mice/group). (C) The ratio of liver weight to body weight of WT mice and USP29-KO mice fed NC chow or HFD diet for 16 weeks (n=8–10 mice/group). (D) Hepatic TG content and (E) serum TG, TC and LDL-C content were detected in WT mice and USP29-KO mice fed NC or HFHC diet for 16 weeks (n=8–10 mice/group). (F) Representative images and relative quantitative statistical analysis of H&E, Oil red O staining of liver tissue from WT and USP29-KO mice fed HFHC diet for 16 weeks (n=6 mice/group). Scale bar, 50 um. (G) Representative images and relative quantitative statistical analysis of CD11b, F4/80, PSR and a-SMA staining of liver tissue from WT and USP29-KO mice fed HFHC diet for 16 weeks (n=4–6 mice/group). Scale bar, 50 um. The data are presented as mean±SD, * indicates a statistical analysis between WT-NC group and WT-HFHC group (** P

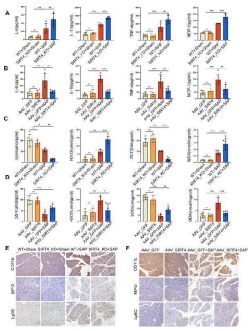

SIRT4 regulated inflammatory response and oxidative stress during SAP in mice. A – B Statistics for the levels of inflammatory factors (IL-6, IL-1beta, TNF-alpha and MCP-1). C – D Statistics for the levels of oxidative stress (GSH, H 2 O 2 , SOD and MDA) in the pancreas of mice. E – F Representative immunohistochemical staining of CD11b, MPO and Ly6G in the pancreas of mice. Scale bar = 100 μm. * P

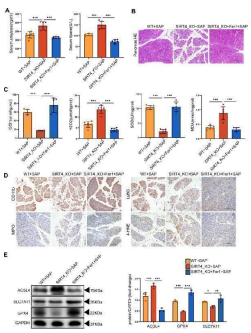

SIRT4 mitigated SAP by suppressing ferroptosis. A Fer-1 decreased the serum amylase level and lipase activity of SAP mice induced by L-Arg. B Representative HE staining images of pancreas. Scale bar = 100 μm. C The levels of oxidative stress (GSH, H 2 O 2 , SOD, MDA) in the pancreas of mice. D Representative IHC staining of CD11b, MPO, Ly6G and 4-HNE in the pancreas of mice in different groups. Scale bar = 100 μm. E The protein expression level of ferroptosis-related proteins (ACSL4, GPX4, SLC7A11) in the pancreas of mice in different groups. WT + SAP group, SIRT4_KO + SAP group, SIRT4_KO+Fer-1 + SAP group. E used GAPDH as the reference protein. * P

RNF5 knockout increased inflammatory response and apoptosis after MI in vivo. (A) Representative images (Left) and quantitative results (Right) of CD11B immunohistochemical staining of heart sections of the two

BOSTER BIOLOGICAL TECHNOLOGY
3942 B Valley Ave, Pleasanton, CA 94566
888-466-3604 | support@bosterbio.com | www.bosterbio.com

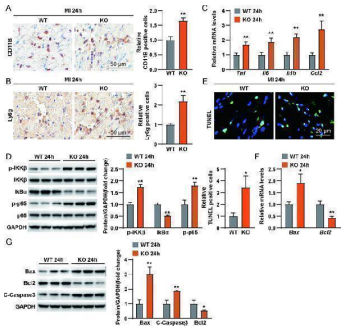

groups of mice (n = 6). Scale bar, 50 um. (B) Representative images and quantitative results of Ly6g immunohistochemical staining of heart sections of the two groups of mice (n = 6). Scale bar, 50 um. (C) RT-PCR results of inflammatory responses associated genes including Tnf , Il6 , Il1b , and Ccl2 in WT and RNF5-KO mice subjected to MI surgery (n = 4). (D) Western blot (Left) and quantification results (Right) of NF-kappaB signaling pathway-related proteins in wild type and RNF5-KO mice subjected to MI surgery (n = 3). GAPDH was used as loading control. (E) Representative images (Up) and quantitative results (Down) of TUNEL staining of mice heart tissues sections from the indicated group (n = 4). Scale bar, 20 um. (F) RT-PCR results of apoptosis-related genes in wild type and RNF5-KO mice subjected to MI surgery (n = 4). The RNA expression levels were normalized to Gapdh . (G) Western blot (Left) and quantification results (Right) of apoptosis-related proteins in wild type and RNF5-KO mice subjected to MI surgery (n = 3). GAPDH was used as loading control. For statistical analysis, a two-tailed Student’s t -test was used. * for p

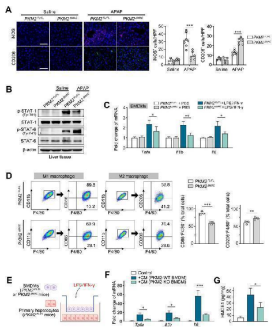

Deletion of PKM2 in macrophages reprogrammed M1 macrophages to M2 macrophages. (A) Representative images and quantification of immunofluorescence staining for iNOS and CD206 in the liver tissues of PKM2 ΔMAC and PKM2 FL/FL mice after 24 h of APAP induction (300 mg/kg). (B) Protein levels of p-STAT1, STAT1, p-STAT6 and STAT6 in liver tissues of PKM2 ΔMAC and PKM2 FL/FL mice induced by APAP or saline. (C) The mRNA levels of Tnfa , Il1b and Il6 in BMDMs of PKM2 ΔMAC and PKM2 FL/FL mice treated with or without LPS/IFN-gamma. (D) Flow cytometry analysis of total macrophages (F4/80 + CD11b +) and M1 (F4/80 + CD11b + CD86 +) macrophages from BMDMs treated with LPS/IFN-gamma, along with analysis of total macrophages (F4/80 + CD11b +) and M2 (F4/80 + CD11b + CD206 +) macrophages from BMDMs treated with IL-4 in vitro . (E) Schematic diagram illustrating the co-culture system of BMDMs and primary hepatocytes of indicated mice in the presence of LPS/IFN-gamma. (F) The mRNA levels of Tnfa , Il1b and Il6 of hepatocytes co-cultured with indicated BMDMs. (G) The levels of HMGB1 in hepatocytes co-cultured with indicated BMDMs. Scale bar: 100 um * P < 0.05; ** P < 0.01; *** P < 0.001. Error bars depict the standard deviations. BMDMs, bone marrow-derived macrophages. PMID: 40351417

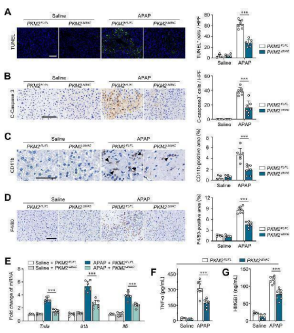

Macrophage PKM2 knockout mice showed ameliorated hepatic inflammation and hepatocyte apoptosis. (A, B) Representative images and quantification of TUNEL staining (A) and immunohistochemistry staining for Cleaved Caspase 3 (B) of PKM2 ΔMAC and PKM2 FL/FL mice after 24 h of APAP induction (300 mg/kg). (C, D) Representative images and quantification of immunohistochemistry staining for CD11b (C) and F4/80 (D) of PKM2 ΔMAC and PKM2 FL/FL mice after 24 h of APAP induction (300 mg/kg). Black arrow indicates CD11b + cells. (E) The mRNA levels of Tnfa, Il1b, Il6 in liver

BOSTER BIOLOGICAL TECHNOLOGY
3942 B Valley Ave, Pleasanton, CA 94566
888-466-3604 | support@bosterbio.com | www.bosterbio.com

tissues of PKM2 ΔMAC and PKM2 FL/FL mice with or without APAP treatment. (F, G) The levels of TNF-alpha (F) and HMGB1 (G) in serum of PKM2 ΔMAC and PKM2 FL/FL mice with or without APAP treatment. Scale bar: 100 um. *** P < 0.001. Error bars depict the standard deviations.Index in PubMed under a CC BY license. PMID: 40351417

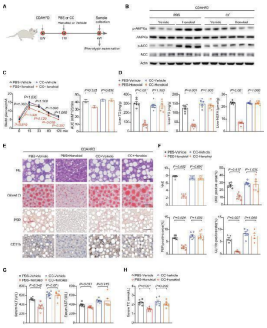

AMPK activation is required for honokiol-mediated beneficial effects in vivo. A Schematic of the experimental procedure used with mice fed a CDAHFD diet and treated with vehicle or honokiol (100 mg/kg) in the absence or presence of compound C (CC, 10 mg/kg, every other day, i.p.). B Western blots of p-AMPKalpha, AMPKalpha, p-ACC, and ACC of mice in the indicated groups. n = 3 mice per group. C The blood glucose concentration during GTT of CDAHFD-fed mice in the indicated groups. n = 6 mice per group. One-way ANOVA was applied for statistical analysis. P -values of the red color represent the comparison of PBS-vehicle vs PBS-honokiol, while black represents CC-vehicle vs CC-honokiol. D Liver contents of TG, TC, and NEFA of CDAHFD-fed mice in the indicated groups. n = 6 mice per group. The Kruskal–Wallis test was applied for statistical analysis. E Representative images of the indicated mouse liver sections stained with HE, ORO, PSR, and IHC for CD11b-positive cells. n = 6 mice per group. Scale bar, 50 um. F Results of NAS (HE) and quantitative analysis of ORO, PSR, and CD11b data shown in (E). n = 6 mice per group. For statistical analysis, the Kruskal–Wallis test was used for NAS and one-way ANOVA was applied to ORO, PSR, and CD11b data. G Serum ALT and AST activity of CDAHFD-fed mice shown in the indicated groups. n = 6 mice per group. Student's t -test was applied for statistical analysis. H Serum TC concentrations in CDAHFD-fed mice treated with the indicated groups. n = 6 mice per group. Student's t -test was applied for statistical analysis. I Dot plot representing pairwise GSVA comparisons of transcriptomic data from CDAHFD-fed mice shown in the indicated groups. J Heatmap of transcriptomic data from CDAHFD-fed mice shown in the indicated groups Index in PubMed under a CC BY license. PMID: 36932412

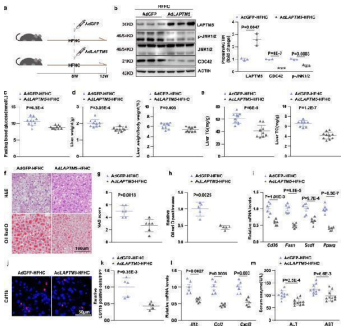

Adenovirus-mediated hepatic Laptm5 over-expression alleviated non-alcoholic steatohepatitis. a Scheme of constructing Ad LAPTM5 -mediated therapeutic NASH models in HFHC mice. b Represents the WB detection results of the proteins indicated in the groups (n = 3 mice/group). c and d Fasting blood glucose (c), liver weight, and LW/BW (d) of mice in the indicated groups (n = 10 mice/group). e Hepatic TG and TC contents of mice in the indicated group (n = 10 mice/group). f H&E (upper) (n = 6 mice/group) and Oil Red O (lower) (n = 5 mice/group) staining in the liver sections. Scale bar, 100 um. g NAS score analysis of the group in panel (f) (n = 6 mice/group). h Statistical analysis of Oil red O in the group of the panel (f) (n = 5 mice/group). i Relative mRNA levels of genes related to the fatty acid metabolism in the livers of mice in the indicated groups (n = 6 mice/group). j and k Immunofluorescence staining (j) and Statistical analysis (k) of CD11b (red) in the liver sections of HFHC-fed mice in the indicated groups (

BOSTER BIOLOGICAL TECHNOLOGY
3942 B Valley Ave, Pleasanton, CA 94566
888-466-3604 | support@bosterbio.com | www.bosterbio.com

n = 5 mice/group). Scale bar, 50 um. l Relative mRNA levels of pro-inflammatory genes in the livers of mice in the indicated groups (n = 6 mice/group). m Serum ALT and AST concentrations of mice in the indicated groups (n = 10 mice/group). Data are represented as mean ± SD, two-tailed Student's t -test was used to evaluate differences in all panels. Source data are provided as a Source data file. Index in PubMed under a CC BY license. PMID: 37156795

1 Publications Citing This Product

1. PubMed ID: 28100749, Promoted interaction of C/EBP%u03B1 with demethylated Cxcr3 gene promoter contributes to neuropathic pain in mice

Visit bosterbio.com/anti-cd11b-rabbit-monoclonal-antibody-m00144-1-boster.html to see all 1 publications.

Anti-CD11b ITGAM Rabbit Monoclonal Antibody

For Research Use Only. Not for use in diagnostic procedures.